AFOSR Award No. FA9550-16-1-0013 and EPSRC EP/N018680/1

Imperial College London

Exploring Wavelength Dependence in Laser Plasma Accelerators

Annabel E Gunn*, Nicholas H Stuart, Stuart P D Mangles, Roland A Smith
Blackett Laboratory, Imperial College London, South Kensington Campus, London SW7 2AZ, UK.

CHIMERA

1. Abstract

In laser wakefield acceleration (LWFA) experiments at major facilities, emphasis is typically placed on "standard" laser and gas parameters such as pulse duration, spot size, normalised vector potential, gas constituents and gas density in order to produce the most stable, high charge, high energy, narrow spread electron beams. While these parameters are certainly of unquestionable importance, the role of the most fundamental laser parameter, its wavelength, remains relatively unexplored. A long wavelength driving laser may be advantageous to a laser wakefield accelerator; both theoretically from scaling laws derived from the ponderomotive force, and from some early simulation results using particle-in-cell codes. Here we present simulation results and further discuss the experimental and theoretical implications of using long wavelength, short pulse drivers in LWFA experiments, with particular emphasis on the high intensity, short pulse, multi-beam mid-infrared (3.7μm central wavelength) Chimera laser system, currently under active development at Imperial College London.

2. Wavelength dependence in Laser Wakefield Accelerators

Laser wakefield acceleration operates over a multi-dimensional phase space, where many of these variables have a wavelength dependence. From Lu *et al.* (2007) [1], the relevant relationships are as follows:

- **Accelerating (ponderomotive force):** $F_{pond} \propto a_0^2 \propto \lambda_L^2$
- **Critical density:** $n_c \propto \frac{1}{\lambda_L^2}$
- **Dephasing & pump depletion lengths:** $L_d, L_{pd} \propto \lambda_L$ (Assuming constant $a_0 = 2$ and constant ${}^{n_e}/_{n_c} = 0.04$)
- **Maximum electron energy gain:** $E_{max} \propto a_0 n_c \propto \frac{1}{\lambda_L}$
- **Number accelerated electrons:** $N_e \propto \lambda_L$

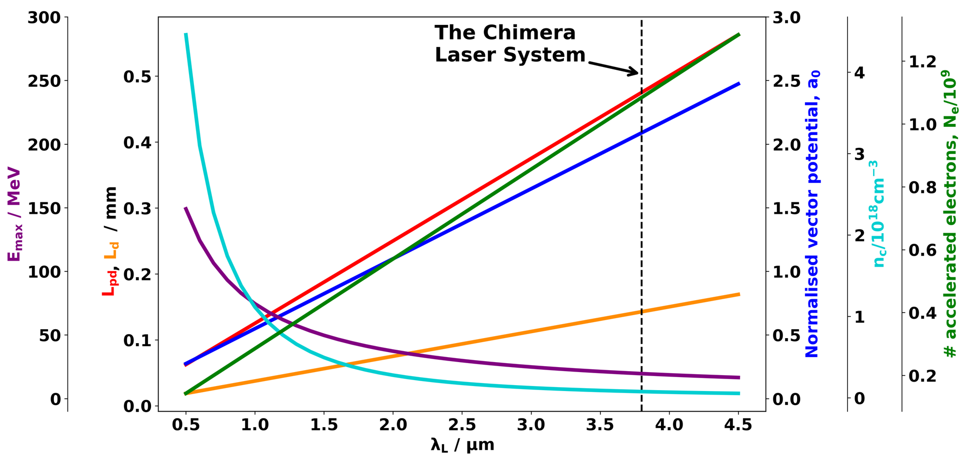

Figure 1: A plot to show relationships between important LWFA parameters, E_{max}, L_d, L_{pd}, a_0, n_c and N_e with driving laser wavelength λ_L. This assumes laser parameters of laser energy $E_L = 25mJ$, beam waist $w_0 = 14.2\mu m$ and pulse duration $\tau_L = 30fs$. Note that in the scalings of L_d and L_{pd}, we assume constant $a_0 = 2$ and constant ${}^{n_e}/_{n_c} = 0.04$.

3. The Chimera Laser System

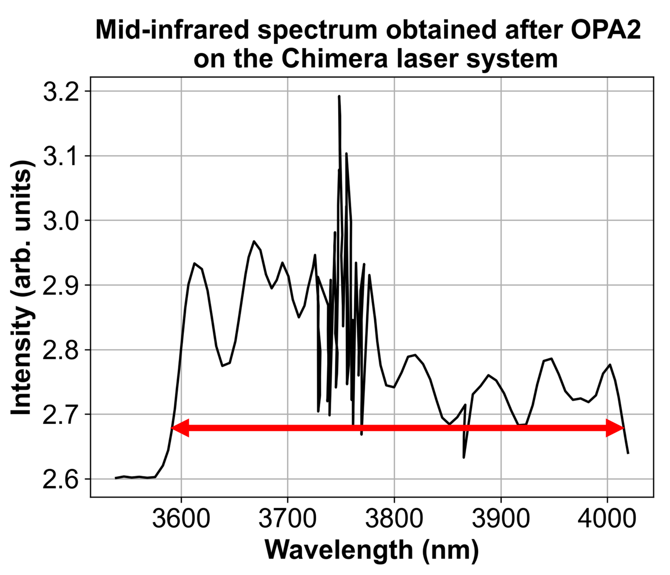

Figure 2: A spectrum taken at the output of the second mid-infrared OPA on the Chimera laser system. The central feature is due to some damage on the detector. The full width at half maximum at this stage is already ~400nm.

Currently under active development at Imperial College London, the Chimera laser system is a high intensity ($\sim 4\times10^{17}$ W/cm^3), few-cycle, short-pulse (~ 3 cycles at 50fs) multibeam laser system, with its main beam centred in the mid-infrared (MIR) spectral range at 3.7μm and an operational bandwidth of ~ 1μm. It is this beam we plan to use to drive a LWFA experiment. Chimera uses 9 cascaded non-linear processes to generate and amplify a few cycle MIR pulse, with difference frequency generation used to initially produce the main MIR beam and optical parametric amplification to latterly amplify it.

The current energy record on this system is a 31mJ, 100fs (uncompressed) 3.7μm signal, detected at the output of the final OPA stage. Similar worldwide systems include a 3.9μm, 30fs, 30mJ system in Austria [2], a 3.3μm, 30mJ, 70fs system in Japan [3] and a 4μm, 2.6mJ, 22fs system in China [4].

4. LWFA Simulations for the Chimera Laser System

In order best exploit a LWFA experiment on the Chimera laser system, we should aim to predict and understand what magnitude of electrons energies we might detect.

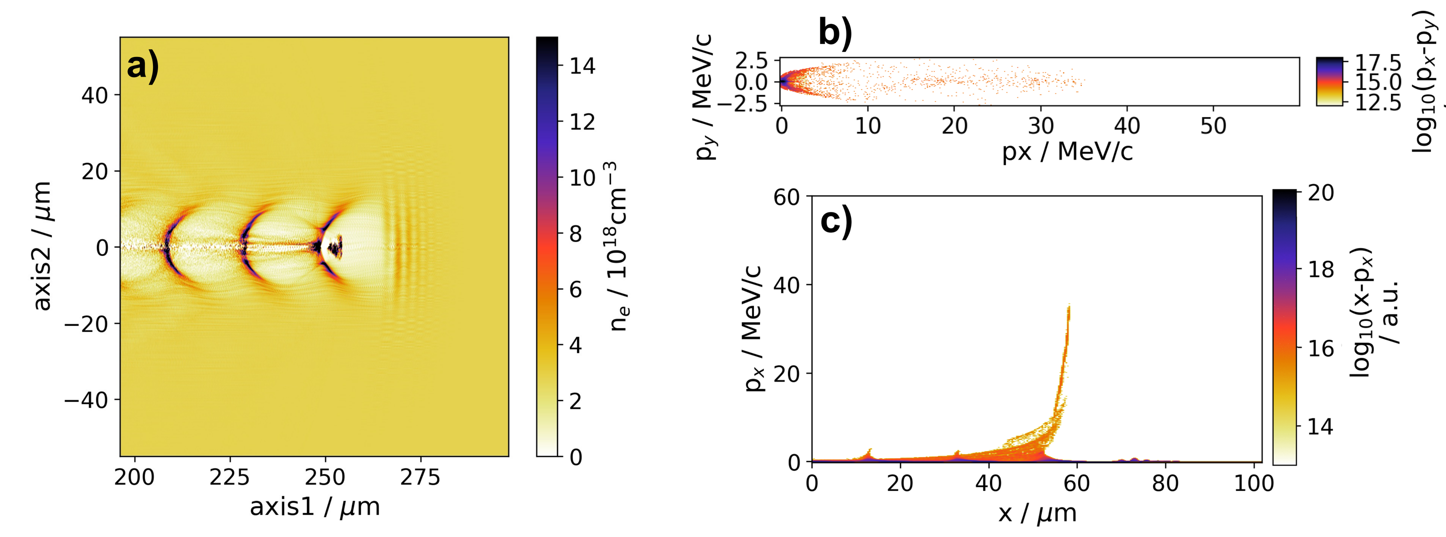

Figure 3: Results of particle-in-cell simulation using a 2 mode azimuthal mode (AM) cylindrical geometry at simulation time of 1.04ps. The plasma density of the simulation is $n_e = 2.8\times10^{18}cm^{-3}$, the normalised vector potential a_0 is 2.0. a) shows plasma density n_e, b) is the $p_x - p_y$ momentum phase space, c) is the $x - p_x$ momentum phase space and d) is the $y-p_y$ momentum phase space

Here we use the particle-in-cell code Smilei using a 2 mode azimuthal mode (AM) cylindrical geometry. The spatial and temporal resolutions in this geometry are $\mathrm{dx} = \mathrm{wavelength}/100$, $\mathrm{dr} = \mathrm{wavelength}/20$, $\mathrm{dt} = 0.96 \times \mathrm{dx}$.

We can scan through a range of plasma densities, collect maximum accelerated electron energies and compare them to theoretical predictions using a couple of different assumptions. Eq. 1 assumes no laser or pre-injection pulse evolution (PIPE), Eq. 2 considers laser evolution but not PIPE, and Eq. 3 attempts to consider both laser evolution and PIPE. These models along with results of a parameter scan of plasma density are shown Figure 4. This plot also includes a model of the predicted self-injection threshold of the laser wakefield accelerator (Eq. 4), using a model proposed by Mangles et al., (2012) [5].

5. Problems with the models

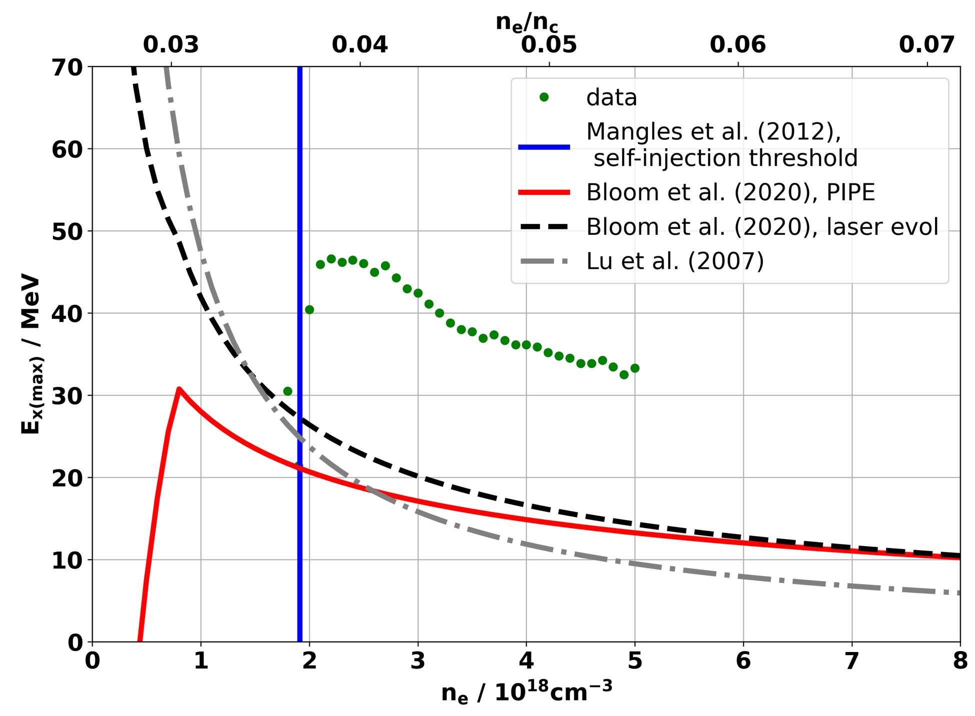

Figure 4: Maximum electron longitudinal energy with plasma densities $n_e = 1.8 - 5.0\times10^{18}cm^{-3}$.

1. **Lu *et al.*, (2007) [1] :**

$$\frac{E_{max}}{m_e c^2} = \frac{2}{3} a_0 \frac{n_c}{n_e}$$

2. **Bloom *et al.*, (2020) [6] :**

$$E'_{max} / m_e c^2 = \frac{4}{3} [{}^{\alpha E_L}/_{\tau_f P_c}]^{1/3} \frac{n_c}{n_e}$$

3. **Bloom *et al.*, (2020) [6] :**

$$E''_{max} = E'_{max}(2\Delta_{acc} - \Delta_{acc}^2)$$

Where $\Delta_{acc} = \frac{(L_{max} - L_{PIPE})}{L_d}$

4. **Mangles *et al.*, (2012) [5] :**

$$\frac{\alpha P}{P_c} > \frac{1}{16}[\ln \frac{2n_c}{3n_e} - 1]^3$$

The theoretical models as shown in Figure 4 clearly do a bad job. The next step here is to understand what phenomena we are missing in this regime.

Direct laser acceleration (DLA) is a mechanism that can cause significant energy gain of accelerated electrons in the bubble regime of a laser wakefield accelerator. This phenomena is one in which accelerated electrons are transferred energy not only from the substantial longitudinal accelerating fields within the wake of laser (LWFA), but also from the laser field itself (DLA). This could be an explanation for the significant mismatch of observed electron energies with theory, as the models used here do not consider any contribution from DLA.

DLA has a characteristic signature in electron momentum space: it exhibits a forked structure in its momentum phase space. If present, this is something we would expect in an electron spectrum. This is not something we see in Figure 3b)..

Particle Tracking can be used to identity particle specific quantities, as opposed to simulation wide macro-quantites. Figure 5 shows the tracks in momentum space of 3 randomly selected electrons trapped in the wake of the laser pulse. Again, if DLA was present, we would expect to see significant transverse electron oscillations: this is not something we observe.

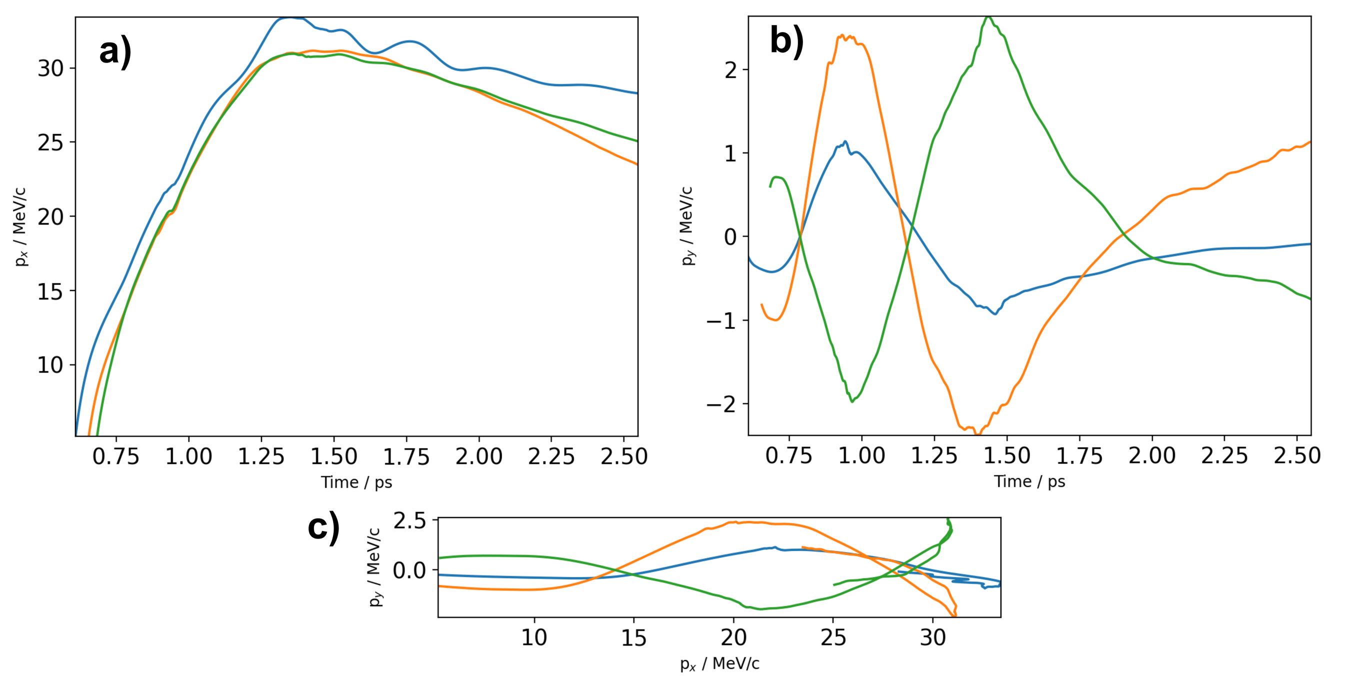

Figure 5: Particle Tracking of 3 random trapped electrons at the end of the simulation (2.55 ps). Note the different scales. a) shows longitudinal momentum p_x in time, b) shows transverse momentum p_y in time c) shows the $px - p_y$ tracks at the end of the simulation.

To understand quantitatively from which mechanism the electrons are receiving their energy we should specifically evaluate the energy gains due to the respective transverse ($E_\perp$) and longitudinal ($E_\parallel$) fields. The energies can be calculated by:

$$W_\parallel = -e \int_0^t E_\parallel \cdot v_\parallel dt$$

$$W_\perp = -e \int_0^t E_\perp \cdot v_\perp dt'$$

Where $E_\parallel$, $E_\perp$, $v_\parallel$ and v refer to the respective longitudinal and transverse electric fields and electron velocities and *e* is electric charge.

6. Discussion & Conclusions

From a qualitative perspective, it does not appear as though DLA is having a major effect on these simulations, however more quantitative work must be done to say this conclusively. From our qualitative evidence, we would expect a plot of the relative contributions of DLA and LWFA to the total energy gain of the electrons to be vastly different. We would expect the LWFA contribution to have a close to linear relationship to the overall electron energy gain, while the DLA contribution would be negligible.

The next step is to think about what mechanism could be causing this discrepancy in electron energies. One possibility is that the red shifting of the laser through the plasma is enhanced due to long wavelength and therefore further enhancing a_0.

[1] W. Lu *et al.*, Phys. Rev. ST Accel. Beams, 10, 061301 (2007), [2] G. Andriukaitis *et. al.*, Opt. Lett. 36, 2755-2757 (2011), [3] Y. Fu *et al.*, Appl. Phys. Lett. 112, 241105 (2018), [4] P. Wang, *et. al.*, Opt. Lett. 43, 2197-2200 (2018), [5] S. P. D. Mangles et al., Phys. Rev. ST Accel. Beams, 15, 011302 (2012), [6] M. S. Bloom *et al.*, Phys. Rev. Accel. Beams, 23, 061301, (2020)

*a.gunn21@imperial.ac.uk

MURI MIR
MID-INFRARED STRONG-FIELD INTERACTION

ACKNOWLEDGEMENT - This poster presentation has received support from the European Union's Horizon 2020 Research and Innovation programme under Grant Agreement No 101004730.

EUROPEAN NETWORK FOR NOVEL ACCELERATORS
EuroNNAc4
NPACT supported by EU via I-FAST

iFAST